View Online / Journal Homepage / Table of Contents for this issue
Dynamic Article Links

Soft Matter

Cite this: *Soft Matter*, 2012, **8**, 1492

www.rsc.org/softmatter

PAPER

Spherical indentation testing of poroelastic relaxations in thin hydrogel layers

Edwin P. Chan,*[a] Yuhang Hu,[b] Peter M. Johnson,[a] Zhigang Suo[b] and Christopher M. Stafford[a]

Received 5th August 2011, Accepted 12th November 2011
DOI: 10.1039/c1sm06514a

In this work, we present the Poroelastic Relaxation Indentation (PRI) testing approach for quantifying the mechanical and transport properties of thin layers of poly(ethylene glycol) hydrogels with thicknesses on the order of 200 μm. Specifically, PRI characterizes poroelastic relaxation in hydrogels by indenting the material at fixed depth and measuring the contact area-dependent load relaxation process as a function of time. With the aid of a linear poroelastic theory developed for thin or geometrically confined swollen polymer networks, we demonstrate that PRI can quantify the water diffusion coefficient, shear modulus and average pore size of the hydrogel layer. This approach provides a simple methodology to quantify the material properties of thin swollen polymer networks relevant to transport phenomena.

Introduction

Thin layers of swollen polymer networks are ubiquitous in various technological applications relevant to sustainability, energy, and bioengineering. Some examples include membranes for water purification,[1,2] proton exchange membranes used in fuel cells,[3,4] scaffolds for tissue engineering,[5] and polymer particles for drug delivery.[6,7] In these examples, their performance is closely linked to the ability to regulate transport of small molecules such as solvent. Hence, understanding the critical time- and length-scales that regulate transport of these molecules within the polymer network provides vital information to enable development of membrane materials with improved performance.

Various techniques including impedence-,[8,9] optical-,[10,11] scattering-,[12] and spectroscopic-based[13–16] measurement approaches have been used to quantify the through-thickness solvent diffusion within swollen polymer network layers. Since the characteristic solvent diffusion time scales with the film thickness squared, this implies that through-thickness diffusion measurements become more challenging for thinner films.

Recently, indentation testing have been demonstrated as an interesting approach to quantify solvent transport in polymer gels.[17–23] An illustrative example is presented in Fig. 1. The approach involves indenting a hydrogel with a spherical probe to a fixed depth (δ) (Fig. 1a). In response to this indentation, a corresponding load develops that is defined by the hydrogel stiffness. As testing time progresses, the hydrogel will undergo a stress-relaxation process (Fig. 1b). Generally, two primary relaxation processes can occur that are related to the dynamics on the polymer chain level. The first process is viscoelastic relaxation, and is associated with conformational changes of the polymer chain due to the applied deformation. The second

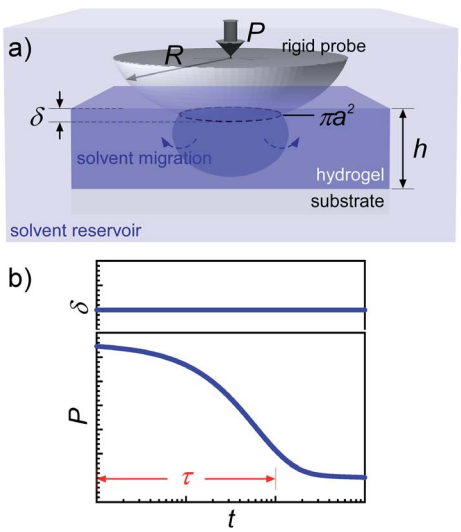

Fig. 1 Spherical indentation testing of relaxation phenomena in hydrogels. (a) A spherical probe is brought into contact with the hydrogel surface in a water environment. The probe-hydrogel and hydrogel-substrate interfaces are considered frictionless. The spherical volume directly beneath the probe represents the hydrogel region where solvent migration occurs. (b) Compressing the gel at a fixed displacement (δ) results in a relaxation in load (P) that is characterized by a relaxation time (τ).

[a]*Polymers Division, National Institute of Standards and Technology, 100 Bureau Drive, Gaithersburg, MD, 20899, USA. E-mail: edwin.chan@nist.gov; Fax: +1 301 975 4924; Tel: +1 301 975 5228*
[b]*School of Engineering and Applied Sciences, Harvard University, Cambridge, MA, 02138, USA. E-mail: suo@seas.harvard.edu; Fax: +1 617 495 9837; Tel: +1 617 495 3789*

process is poroelastic relaxation. This relaxation process is associated with the transport of water molecules out of the region of hydrogel material under deformation as defined by the contact area πa^2. Both processes are concurrent, with each leading to a macroscopic relaxation of the load response. However, the characteristic relaxation time-scale (τ) of each process is unique since the two relaxation times depend on different sets of materials properties.

The viscoelastic relaxation time-scale (τ_R) is determined by the ratio of the shear viscosity (η) and shear modulus (G) of the hydrogel, $\tau_R \sim \eta/G$.[24] Both of these material properties are independent of the contact radius established by a typical millimetre-sized indenter ($a \approx 100$ μm). This implies that τ_R is also independent of the contact size.

On the other hand, the poroelastic relaxation time-scale (τ_P) is proportional to the size of the contact. This contact-size dependence is attributed to the time-scale required for the solvent within the deformed volume of hydrogel material to migrate over a distance defined by the contact radius. Specifically, τ_P is related to the contact radius and the diffusion coefficient (D) of the solvent within the hydrogel by:[18,19]

$$\tau_p \approx \frac{a^2}{D} \quad . \tag{1}$$

Therefore, the time-scales of the two relaxation processes are distinguishable based on the contact size. As an example, for a typical swollen polymer network with parameters of $D = 10^{-10}$ m^2/s and $a = 100$ μm, the poroelastic relaxation time ($\tau_P \approx 100$ s) is significantly longer than its viscoelastic relaxation time ($\tau_R \sim 0.1$ s). More importantly, eqn (1) suggests that we can adjust the poroelastic relaxation time simply by controlling the contact area.

This indentation testing approach is attractive for measuring the material properties of thin swollen polymer networks for several reasons. First, the test measures solvent transport over the lateral dimensions of the polymer film as opposed to the through-thickness dimension. For polymer films with isotropic properties, this measurement approach is not limited by the film thickness of the polymer layer as compared to the other techniques. Second, the approach is quite simple and straightforward to implement since it only involves indenting the material at fixed depth with a macroscopic spherical probe. Therefore, the test facilitates direct measurements of the materials properties of the polymer film that is supported by a substrate. Third, several material properties including diffusion coefficient, shear modulus, and average pore dimension can be extracted directly. We envision adapting this technique for membranes because it can directly measure the poroelastic relaxations of a membrane film and correlate the response to material properties such as diffusivity and average pore dimension.

Although the approach has been demonstrated for thick hydrogel materials, its relevance for thin hydrogel layer and other hydrated polymer membranes have not been explored. Therefore, the objective of this work is to demonstrate Poroelastic Relaxation Indentation (PRI) in quantifying the transport properties for thin or geometrically confined swollen polymer network based on poly(ethylene glycol) (PEG) hydrogel layers.

Materials and methods†

Mechanics of indenting a thin poroelastic layer

Indentation of a highly swollen polymer network, such as a hydrogel, is unique in that the mechanical deformation is coupled to the mass transport of solvent through the network, which is a phenomena known as poroelasticity.[25] This deformation causes a chemical potential gradient to develop within the hydrogel. Over time, the hydrogel establishes a new chemical equilibrium *via* migration of water away from the region under deformation. Due to this diffusion process, the hydrogel undergoes a load relaxation that reflects the time-scale to establish this new equilibrium, which corresponds to the poroelastic relaxation time.

Immediately following indentation, the water molecules do not have sufficient time to migrate away from the deformed region of the hydrogel. Therefore, the hydrogel is considered to be incompressible ($\nu = 0.5$), and the indentation response is equivalent to deformation of an elastic layer. For an elastic film deformed by a spherical probe to an indentation depth δ, the resultant load is defined as:[26]

$$P = P_H \cdot f_P\left(\sqrt{R\delta}/h\right) = \frac{8R^{1/2}\delta^{3/2}G}{3(1-\nu)} \cdot f_P\left(\sqrt{R\delta}/h\right) \quad . \tag{2}$$

where G and ν correspond to the shear modulus and Poisson's ratio of the elastic material, respectively. The parameter P_H is the Hertz load predicted by Hertzian contact mechanics of an elastic layer considered to be semi-infinitely thick in relation to the Hertz contact radius defined as,

$$a_H = \sqrt{R\delta} \quad . \tag{3}$$

Eqn (3) does not provide an accurate description of the contact radius when it becomes commensurate or greater than the hydrogel layer thickness. Here, the contact radius is related to the indentation depth by:

$$a = \sqrt{R\delta} \cdot f_a\left(\sqrt{R\delta}/h\right) \quad . \tag{4}$$

The function $f_a\left(\sqrt{R\delta}/h\right)$ accounts for deviations from Hertz mechanics where the substrate stiffness influences the geometric relationship between contact radius and indentation depth. This function was solved numerically based on the work of Yu and coworkers.[26] Details of this calculation are discussed in a separate contribution.[27] The approximate analytical form is:

$$f_a\left(\sqrt{R\delta}/h\right) = \frac{1.41\left(\sqrt{R\delta}/h\right)^2 + 0.57\left(\sqrt{R\delta}/h\right) + 0.5}{\left(\sqrt{R\delta}/h\right)^2 + 0.49\left(\sqrt{R\delta}/h\right) + 0.5} \quad . \tag{5}$$

Similarly, the function $f_p\left(\sqrt{R\delta}/h\right)$ accounts for the deviation from Hertz load when the stress field is affected by substrate stiffness. We solve this function numerically and details of the numerical calculation are discussed separately.[27] The approximate analytical form is:

† The equipment and instruments or materials are identified in the paper in order to adequately specify the experimental details. Such identification does not imply recommendation by NIST, nor does it imply the materials are necessarily the best available for the purpose.

$$f_P\left(\sqrt{R\delta}/h\right) = \frac{2.36\left(\sqrt{R\delta}/h\right)^2 + 0.82\left(\sqrt{R\delta}/h\right) + 0.46}{\left(\sqrt{R\delta}/h\right) + 0.46} \quad . \tag{6}$$

Hence, the instantaneous load response (P_i) of the hydrogel immediately following indentation is,

$$P_i = \frac{16}{3} R^{1/2} \delta^{3/2} G \cdot f_P\left(\sqrt{R\delta}/h\right) \quad . \tag{7}$$

As time progresses, the solvent molecules migrate from the deformed hydrogel region until a new chemical equilibrium is reached. Due to this transport process, the hydrogel relaxes to an equilibrium or long-time load (P_f) defined by eqn (2).

To model the load relaxation process, we perform finite element calculations using ABAQUS software. In the calculation, the probe indents the hydrogel layer rapidly, with a loading time 10^{-5} times faster than the total relaxation time. Both the probe-hydrogel and hydrogel-substrate interfaces are considered to be frictionless and impermeable. Within the contact area, the water flux is zero along the probe-hydrogel interface. The hydrogel deformation follows the same configuration of the probe. Outside the contact area, the boundaries are traction-free and in diffusive equilibrium with the external water reservoir. To simulate a rigid substrate with a frictionless and impermeable hydrogel-substrate interface, the indentation of the hydrogel layer in vertical direction is constrained and zero flux is established. Details of the calculations are discussed in a separate contribution.[27] The calculations were performed to determine the poroelastic load relaxation behavior for a broad range of $\sqrt{R\delta}/h$ ratios from 0.11 to 2.98 (Fig. 2a). The results are described in terms of a dimensionless load relaxation function g, *versus* dimesionless relaxation time, $Dt/R\delta$:

$$\frac{P(t) - P_f}{P_i - P_f} = g\left(Dt/R\delta, \sqrt{R\delta}/h\right) \quad . \tag{8}$$

The results of Fig. 2a indicate that the shape of the load relaxation curve depends significantly on the degree of geometric confinement as defined by the $\sqrt{R\delta}/h$ ratio. An interesting feature is that the poroelastic relaxation time required to relax from P_i to P_f descreases with increasing $\sqrt{R\delta}/h$ ratio, suggesting that the poroelastic relaxation time for a geometrically confined hydrogel of a given thickness decreases with indentation depth.

To develop an analytical solution that describes the poroelastic relaxation behavior for the $\sqrt{R\delta}/h$ ratios explored, we extrapolate an approximate g function from each curve. We find the g function takes the stretched exponential form, commonly used to describe polymer chain dynamics (Fig. 2b):[28,29]

$$g\left(Dt/R\delta, \sqrt{R\delta}/h\right) = \exp\left(-\alpha(Dt/R\delta)^{\beta}\right) \quad . \tag{9}$$

The parameters α and β (Fig. 2b inset) are related to the $\sqrt{R\delta}/h$ ratios and represented by polynomials defined as:

$$\alpha = 1.15 + 0.44\left(\sqrt{R\delta}/h\right) + 0.89\left(\sqrt{R\delta}/h\right)^2 - 0.42\left(\sqrt{R\delta}/h\right)^3 + 0.06\left(\sqrt{R\delta}/h\right)^4 \quad , \tag{10}$$

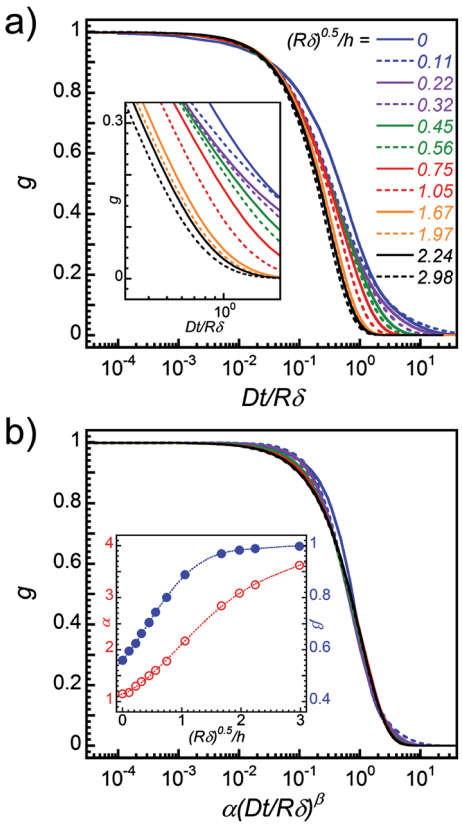

Fig. 2 (a) Finite element calculations of the poroelastic load relaxation function g, for hydrogel layers at different $\sqrt{R\delta}/h$ ratios. The inset is an enlarge view of the same result. (b) Collapse of the entire set of g functions with a stretched exponential function. The inset plot summarizes the α (unfilled symbols) and β (filled symbols) parameters, which are fitted with polynomial functions as represented by eqn (10) and eqn (11), respectively.

$$\beta = 0.56 + 0.25\left(\sqrt{R\delta}/h\right) + 0.28\left(\sqrt{R\delta}/h\right)^2 - 0.31\left(\sqrt{R\delta}/h\right)^3 + 0.1\left(\sqrt{R\delta}/h\right)^4 - 0.01\left(\sqrt{R\delta}/h\right)^5 \quad . \tag{11}$$

Preparation of PEG hydrogel layers

The PEG hydrogel layers were synthesized by photopolymerizing poly(ethylene glycol) methyl ether methacrylate monomer (*molecular mass* = 475 g/mol, PEGMA), poly(ethylene glycol) dimethacrylate crosslinker (*molecular mass* = 875 g/mol, PEGDMA) (Sigma-Aldrich, St. Louis, MO) with de-ionized water, and using 2,2-dimethoxyphenyl acetophenone (DMPA) as the photoinitiator (Irgacure, BASF Corp., Florham, NJ). All chemicals were used as supplied. Monomer formulation containing 90/10% *by mass* of PEGMA/PEGDMA was prepared. DMPA was added (0.5% *by mass*) and allowed to dissolve completely. This formulation was then diluted 50% *by mass* with de-ionized water before polymerization.

To polymerize hydrogel layers of defined film thicknesses, the monomer formulation was filled between two glass substrates with spacers ranging between 150 μm to 2000 μm. Photopolymerization was conducted using a Novacure 2000 ultraviolet

mercury arc lamp (EXFO, Mississauga, ON) at a light intensity of 10 mW/cm^2 for 1200 s. The samples were delaminated from the glass substrates and immediately immersed into de-ionized water. Samples swelled to an equilibrium state and remained in 23 °C water for 48 h prior to testing. Water was periodically replaced to remove any low molecular mass species which could diffuse out of the hydrogel. The thicknesses of the hydrogels were determined by measuring film cross sections *via* optical microscopy prior to testing. The thicknesses of PEG hydrogel layers investigated were 2682 μm ± 7 μm, 1338 μm ± 5 μm, and 267 μm ± 7 μm.

Poroelastic Relaxation Indentation (PRI)

Next, we measure the poroelastic relaxations of the hydrogel layers using PRI. This test monitors the load relaxation, P, of the hydrogel as a function of time due to an indentation depth, δ, with a spherical probe. Since the testing mode is a displacement-controlled type, the indentation depth, and therefore the contact area remains fixed over the entire test.

The PRI measurement approach is illustrated in Fig. 1a. First, an equilibrated hydrogel layer is transferred into a water reservoir enclosure, and is allowed to dwell for 1 h prior to testing. Next, a rigid glass probe with radius of curvature R (=5 mm) is brought into contact with the hydrogel surface at a constant indentation rate (=20 μm/s) to a predefined indentation depth that is controlled by a nanopositioner. During the entire test, the indentation depth and load are monitored by a fiber optic displacement sensor and load cell, respectively. Each hydrogel sample was indented at several different depths. Depending on the indentation depth and hydrogel layer thickness, PRI test can span from 15 min to 2 h. The test is complete when the load relaxation has reached a long-time steady-state value.

Representative PRI testing results for the 1338 μm thick PEG hydrogel are shown in Fig. 3. Upon indenting the hydrogel to a depth δ, an instantaneous load P_i is reached. As testing time progresses, poroelastic relaxation is observed, which is characterized by a time-dependent relaxation of the instantaneous load. Eventually, the load reaches a steady-state lower limit, which is defined as the long-time load P_f. By indenting to greater depths, the magnitude of the instantaneous and long-time load, along with the poroelastic relaxation time, will change as defined by eqn (2), eqn (7) and eqn (9), respectively.

The water diffusion coefficient is determined by constructing a master curve defined by eqn (9). The approach is identical to the procedure used to collapse all the g functions from the finite element calculations into a single master curve (Fig. 2b). First, the results from the PRI tests are converted to dimensionless load $g = ((P - P_f)/(P_i - P_f))$ *versus* adjusted time ($t/R\delta$) curves. Then, the α and β coefficients for each PRI test are determined based on the experimentally defined $\sqrt{R\delta}/h$ ratio. Finally, a best fit of each dimensionless load *versus* dimensionless relaxation time curve is obtained using eqn (9) with the diffusion coefficient D as the lone fitting parameter. As shown in Fig. 3b, all the resultant curves collapse onto a master curve.

Mass swelling ratio. Mass swelling ratios of the PEG hydrogel layers were determined from the ratio of the equilibrium wet mass to dry mass. The wet mass of approximately of 1 g equilibrated PEG hydrogel was measured in air. The samples were then dried for 72 h under vacuum, and the dry mass measured. The calculated swelling ratios were invariant to the hydrogel thickness.

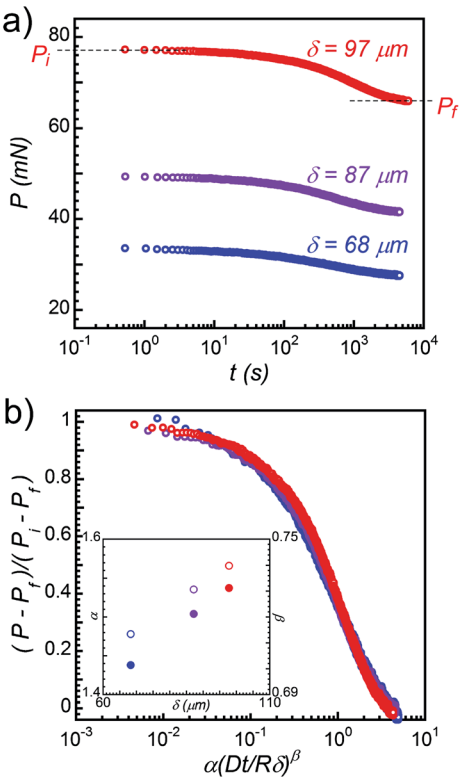

Fig. 3 (a) Representative PRI testing results for the 1338 μm thick PEG hydrogel. The test applies a constant deformation by indenting the hydrogel with a spherical probe at a fixed indentation depth (δ). This indentation process results in a relaxation in load (P) as a function of time (t). The poroelastic relaxation process is characterized as the time required by the hydrogel to relax from P_i to P_f in order to establish a new chemical equilibrium. (b) Extrapolation of the water diffusion coefficient by normalizing the relaxation load *versus* time curves into dimensionless load *versus* dimensionless time curves. This approach is identical to the approach shown in Fig. 2b. By fitting all the curves with eqn (9), the diffusion coefficient can be determined for each test. The inset plot summarizes the α and β coefficients for each test, which depend on the degree of geometric confinement defined by $\sqrt{R\delta}/h$.

Results and discussion

We used the poroelastic model to determine the materials properties of the thin hydrogel layers. Since PRI couples contact mechanics to fluid transport, both the mechanical and transport properties of the hydrogel can be obtained with this one testing method to quantify the hydrogel shear modulus and the water diffusion coefficient separately.

First, we quantify the shear modulus of the hydrogel layers. At instantaneous time when water cannot migrate and the hydrogel is considered to be incompressible, the PRI test is equivalent to the contact mechanical testing of an elastic solid. In contact mechanical testing, the shear modulus is determined in a straightforward manner by extrapolating the value from the

load-indentation depth curve, thus a series of instantaneous load *versus* indentation depth data points obtained from PRI is equivalent to a load *versus* displacement curve from a contact mechanical test.[30] Here, the shear modulus of the PEG hydrogels is determined from the instantaneous load *versus* indentation depth results of the PRI tests.

Specifically, we used eqn (7) to determine the shear modulus for all the hydrogel layers based on the set of P_i, δ values obtained from the PRI experiments (Fig. 4a). The average shear modulus is, $G = 1.0 \times 10^5$ N/m^2 $\pm$ 1.5×10^4 N/m^2, which is within the range for similar types of PEG hydrogels.[31,32]

The water diffusion coefficients are determined using the procedure outlined in the Materials and Methods section. As summarized in Fig. 4b, the average water diffusion coefficient is, $D = 4.4 \times 10^{-10}$ m^2/s $\pm$ 7.6×10^{-11} m^2/s, which is in good agreement with reported values for a crosslinked PEG diacrylate/PEG acrylate hydrogel with similar water content ($D = 4.8 \times 10^{-10}$ m^2/s).[33]

The material properties obtained from PRI testing can be linked with the molecular structure of the hydrogel that governs transport if we consider the diffusion of water through the hydrogel network is analogous to flow through a pore with an average size ξ_P.[34]

In this case, the average pore size is proportional to the hydrodynamic permeability. In relation to poromechanics of hydrogels, the average pore size is related to the materials constants that can be experimentally measured from PRI testing (D,G,ν). Specifically, the pore size is defined as:[19]

$$\xi_P = 2\left(\frac{\eta}{2}\frac{D(1-2\nu)}{G(1-\nu)}\right)^{1/2}, \qquad (12)$$

where η is the viscosity of water.

The Poisson's ratio is also determined by the PRI experiments. Traditionally, Poisson's ratio describes the compressibility of a material due to mechanical deformation. Here, the change in compressibility is due to the fact that the water content within the deformed region is not conserved during PRI testing. Thus, this change in Poisson's ratio should be considered as a change in solvent volume fraction. Specifically, this parameter is related to the ratio of the instantaneous and long-time loads, $P_i/P_f = 2(1-\nu)$ as defined by eqn (2) and eqn (5).[17,18] Rearranging this expression leads to the following:

$$P_f - P_i/2 = \nu\, P_f \qquad (13)$$

We use eqn (13) to determine the average value of the Poisson's ratio by plotting $P_f - P_i/2$ *vs.* P_f (Fig. 5) of all the hydrogel layers. From the slope of the curve, we find $\nu = 0.43$. Substituting this value, along with the other materials constants for the hydrogel and water ($\eta \approx 10^{-3}$ N·s/m^2),[35] we determine $\xi_P \approx 1.5$ nm.

From the swelling ratio measurements of the hydrogel layers, a volumetric swelling ratio, $S \approx 5$, is obtained. Based on a modified Flory–Rehner theory developed for isotropic swelling of hydrogels, the average pore size of a polymer network is estimated to be:[36]

$$\xi = (S)^{1/3}(2C_nM_c/M_r)^{1/2}\, l \qquad (14)$$

where C_n is the Flory characteristic ratio, the ratio M_c/M_r is the number of C–C bonds between crosslinks, and l is the C–C bond distance. Assuming the following PEG polymer chain constants, $C_n = 3.8$,[37] $M_c/M_r = 725$ g mol^{-1}/44 g mol^{-1} $\approx$ 16,[38] and $l = 1.54$ Å, we find $\xi \approx 2$ nm. We note that the hydrogel network model used in eqn (14) assumes that the polymer chains between network junctions consist of linear homopolymer chains, whereas the PEG hydrogels used in this work consist of essentially co-monomers. Thus, eqn (14) can only be used as an estimation of the average pore size. Nevertheless, the pore size determined by both techniques are in close agreement, thus demonstrating that the PRI technique can be used to estimate an average pore dimension of the PEG hydrogel.

Conceptually, it is reasonsable to expect that the contact radius defines the primary length-scale that determines the poroelastic relaxation time irrespective of the hydrogel layer thickness. This concept can be demonstrated by comparing the PRI testing of a thick, or geometrically unconfined ($a \ll h$) and

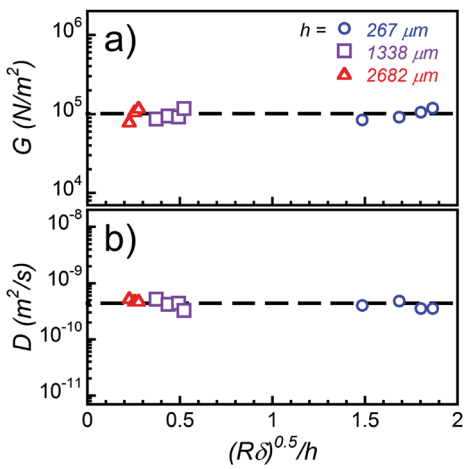

Fig. 4 Summary of materials properties obtained by PRI testing. (a) Shear modulus of the PEG hydrogel as a function of the degree of geometric confinement for all the hydrogel layers. (b) Diffusion coefficient of water as a function of the degree of geometric confinement for all the hydrogel layers. The dashed lines represent the average modulus and diffusion coefficient determined from the PRI tests. The error bars, which are smaller than the symbol size, represent one standard deviation.

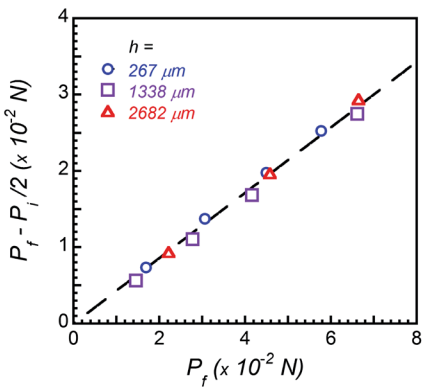

Fig. 5 Determination of the Poisson's ratio upon complete relaxation of the load. By plotting $P_f - P_i/2$ *vs.* P_f of all the hydrogel layers, the slope of the curve defines the average value of the Poisson's ratio, $\nu = 0.43$.

a thin, or highly geometrically confined ($a > h$) hydrogel layer (Fig. 6).

In both cases, the indentation process deforms a volume of hydrogel material (V) that is related to the size of the contact radius. This volume is approximately $V \sim a^3$ and $V \sim a^2h$, for the thick and thin hydrogel layers, respectively. In response, the hydrogel layers relieve the deformation *via* water migration away from the region of indentation. Specifically, a volume of water must migrate over a surface area (A_s) that is also defined by the shape of the deformed region. This surface area is approximately $A_s \sim a^2$ and $A_s \sim ah$, for the thick and thin hydrogel layers, respectively. Regardless of the hydrogel layer thickness, the volume defines the amount of water that will migrate while the surface area defines the time-scale of water migration. The volume-to-surface area ratio defines the lateral length-scale for solvent transport through the hydrogel during PRI testing. Thus, this primary length-scale, as defined by a, determines the average characteristic time-scale of the poroelastic relaxation process.

Finally, Fig. 6 also qualitiatively explains the finite-element predictions of Fig. 2 where we find that the average poroelastic relaxation time decreases with increasing geometric confinement. More importantly, the β coefficient, which describes the breadth of the distribution of poroelastic relaxation time, approaches unity with geometric confinement. This trend is associated with the relationship between pressure distribution and geometric confinement. According to Darcy's law, the pressure distribution is directly proportional to water migration. Since the load relaxation process measured by PRI provides an indirect measure of transport, any change in the pressure distribution, such as the extent of geometric confinement, will lead to changes in the poroelastic relaxation process. In the geometrically unconfined case, the pressure distribution is spherical due to the shape of the probe and absence of substrate stiffness effect (Fig. 6a). As a result, water migration will be different depending on the location of the water molecules within the deformed hydrogel region. At the other extreme of highest geometric confinement, the pressure distribution has a more cylindrical or uniform profile due to substrate stiffness effect (Fig. 6b). Here, the uniform pressure distribution implies that water migration will be independent of location within the deformed hydrogel. The observation that the β exponent (eqn (9)), typically used to describe the distribution of relaxation times in polymer dynamics, approaches unity as $\sqrt{R\delta}/h$ increases supports this concept that the breadth in the distribution of water migration times narrows with geometric confinement.

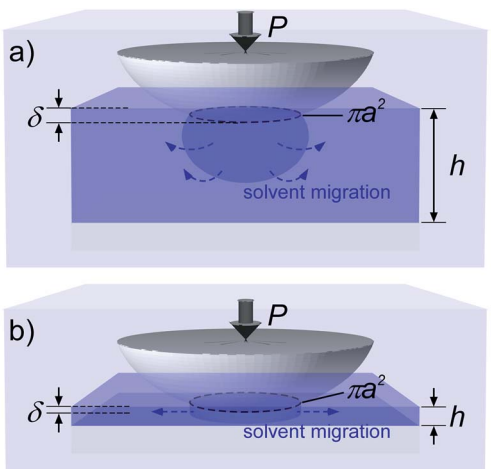

Fig. 6 Comparison of the PRI testing of (a) semi-infinitely thick hydrogel where the contact radius is significantly less than the layer thickness ($a \ll h$) and (b) thin film case where the contact radius is greater than the layer thickness ($a > h$). The volume directly beneath the probe represents the hydrogel region where solvent migration occurs.

This result has important implications from a measurement standpoint. Unlike other techniques for measuring diffusion, PRI is not limited by the thickness of the polymer layer since it is measuring lateral diffusion as opposed to through-thickness diffusion. Additionally, the time-scale of the test is determined by the contact radius, which is experimentally controlled by the indentation depth. Therefore, coupling with other relaxation processes can be avoided because the time-scale for poroelastic relaxation can be adjusted. Since PRI testing couples contact mechanics to fluid transport, the indentation profile will determine the migration behavior of the solvent. Thus, the key assumption for extracting the materials properties from PRI is that the mechanical and transport properties of the polymer layer of interest are considered to be isotropic.

Conclusions

We have demonstrated PRI as an alternative and simple testing approach for characterizing the transport properties of thin PEG hydrogel layers. By utilizing a linear poroelastic theory that predicts the relaxation response over a range of geometric confinement from unconfined to highly confined, the results from PRI testing enable determination of three materials properties of the hydrogel including shear modulus, diffusion coefficient, and average pore dimensions.

In the highly geometrically confined scenario, the PRI approach is quantifying the lateral diffusion process. In theory, PRI is not limited by the thickness of the polymer layer. The important aspects to consider are: (1) the materials properties (D, G) of the polymer are assumed to be isotropic, and (2) the contact radius is sufficient large to avoid overlapping with other relaxation time-scales, which can be accomplished via increases in R or δ. While this work has demonstrated that PRI can measure the transport for "thin" or geometrically confined hydrogel layers, more work is needed to show that the technique can measure thinner polymer layers such as membranes used in water purification. Additionally, we are interested in imaging the deformed region of the hydrogel during PRI testing to validate the poroelastic process as a function of geometric confinement.

Another point we would like to make is that many polymers gels behave as hyperelastic materials at large strains. Thus, a systematic study of the effect of nonlinear strains on their poroelastic relaxation process is warranted. Work is underway to study the effects of nonlinear strains on the poroelastic relaxation of physical gels such as block copolymer photonic gels where their mechanochromic properties are strongly tied to poromechanics.[39]

Finally, based on eqn (1), the poroelastic relaxation time is linked with the diffusion coefficient of small molecules. Therefore, PRI should be capable of measuring the diffusion of

multiple small molecule species within the polymer layer, provided that the diffusion coefficients are unique and the diffusion processes are uncoupled. This measurement can potentially be applicable for quantifying the diffusion of pharmaceuticals within hydrogel-based drug particles. Work is currently underway to characterize the diffusion of water and linear polymer chains within hydrogel layers using PRI.

Acknowledgements

EPC acknowledges the National Research Council for financial support. YH and ZS acknowledge the National Science Foundation (NSF) (CMMI-0800161), Multidisciplinary University Research Initiative (MURI) (W911NF-09-1-0476), and the Materials Research Science and Engineering Center at Harvard University (DMR-0820484). The authors thank Blessing Deeyaa for assistance with the hydrogel deswelling experiments. Official contribution of the National Institute of Standards and Technology; not subject to copyright in the United States.

Notes and references

1 M. A. Shannon, P. W. Bohn, M. Elimelech, J. G. Georgiadis, B. J. Marinas and A. M. Mayes, *Nature*, 2008, **452**, 301–310.
2 G. M. Geise, H.-S. Lee, D. J. Miller, B. D. Freeman, J. E. McGrath and D. R. Paul, *J. Polym. Sci., Part B: Polym. Phys.*, 2010, **48**, 1685–1718.
3 B. C. H. Steele and A. Heinzel, *Nature*, 2001, **414**, 345–352.
4 M. A. Hickner, H. Ghassemi, Y. S. Kim, B. R. Einsla and J. E. McGrath, *Chem. Rev.*, 2004, **104**, 4587–4612.
5 J. L. Drury and D. J. Mooney, *Biomaterials*, 2003, **24**, 4337–4351.
6 B.-S. Kim and J.-W. Choi, *Biotechnol. Bioprocess Eng.*, 2007, **12**, 323–332.
7 S. Kim, J.-H. Kim, O. Jeon, I. C. Kwon and K. Park, *Eur. J. Pharm. Biopharm.*, 2009, **71**, 420–430.
8 V. N. Nguyen, F. X. Perrin and J. L. Vernet, *Corros. Sci.*, 2005, **47**, 397–412.
9 M. G. Penon, S. J. Picken, M. Wubbenhorst and J. van Turnbout, *J. Appl. Polym. Sci.*, 2007, **105**, 1471–1479.
10 J. S. Papanu, D. W. Hess, A. T. Bell and D. S. Soane, *J. Electrochem. Soc.*, 1989, **136**, 1195–1200.
11 Z. Fan and D. J. Harrison, *Anal. Chem.*, 1992, **64**, 1304–1311.
12 B. D. Vogt, H.-J. Lee, V. M. Prabhu, D. M. DeLongchamp, E. K. Lin and S. K. Satija, *J. Appl. Phys.*, 2005, **97**, 114509.
13 I. Linossier, F. Gillard, M. Romand and J. F. Feller, *J. Appl. Polym. Sci.*, 1998, **66**, 2465–2473.
14 C. M. Balik and W. H. SimendingerIII, *Polymer*, 1998, **99**, 4723–4728.
15 S. Deabate, R. Fatnassi, P. Sistat and P. Huguet, *J. Power Sources*, 2008, **176**, 39–45.
16 V. Baukh, H. P. Huinink, O. C. G. Adan, S. J. F. Erich and L. G. J. van der Ven, *Macromolecules*, 2011, **44**, 4863–4871.
17 C.-Y. Hui, Y.-Y. Lin, F.-U. Chuang, K. R. Shull and W.-C. Lin, *J. Polym. Sci., Part B: Polym. Phys.*, 2005, **44**, 359–370.
18 Y.-Y. Lin and B.-W. Hu, *J. Non-Cryst. Solids*, 2006, **352**, 4034–4040.
19 W.-C. Lin, K. R. Shull, C.-Y. Hui and Y.-Y. Lin, *J. Chem. Phys.*, 2007, **127**, 094906.
20 M. Galli, K. S. C. Comley, T. A. V. Shean and M. L. Oyen, *J. Mater. Res.*, 2008, **24**, 973–979.
21 Y. Hu, X. Zhao, J. J. Vlassak and Z. Suo, *Appl. Phys. Lett.*, 2010, **96**, 121904.
22 X. Zhao, N. Huebsch, D. J. Mooney and Z. Suo, *J. Appl. Phys.*, 2010, **107**, 063509.
23 Y. Hu, X. Chen, G. M. Whitesides, J. J. Vlassak and Z. Suo, *J. Mater. Res.*, 2011, **26**, 785–795.
24 M. Rubinstein and R. H. Colby, *Polymer Physics*, Oxford University Press Inc., New York, 2003.
25 G. W. Scherer, *J. Non-Cryst. Solids*, 1989, **109**, 171–182.
26 H. Y. Yu, S. C. Sanday and B. B. Rath, *J. Mech. Phys. Solids*, 1990, **38**, 745–764.
27 Y. Hu, E. P. Chan, J. J. Vlassak and Z. Suo, *J. Appl. Phys.*, 2011, **110**, 086103.
28 G. D. J. Phillies and P. Peczak, *Macromolecules*, 1988, **21**, 214–220.
29 D. J. Plazek and K. L. Ngai, *Macromolecules*, 1991, **24**, 1222–1224.
30 K. R. Shull, D. Ahn, W. L. Chen, C. M. Flanigan and A. J. Crosby, *Macromol. Chem. Phys.*, 1998, **199**, 489–511.
31 S. J. Bryant and K. S. Anseth, *J. Biomed. Mater. Res.*, 2001, **59**, 63–72.
32 S. Lin-Gibson, S. Bencherif, J. A. Cooper, S. J. Wetzel, J. M. Antonucci, B. M. Vogel, F. Horkay and N. R. Washburn, *Biomacromolecules*, 2004, **5**, 1280–1287.
33 H. Ju, A. C. Sagle, B. D. Freeman, J. I. Mardel and A. J. Hill, *J. Membr. Sci.*, 2010, **358**, 131–141.
34 G. W. Scherer, *Langmuir*, 1996, **12**, 1109–1116.
35 J. Kestin, M. Sokolov and W. A. Wakeham, *J. Phys. Chem. Ref. Data*, 1978, **7**, 941–948.
36 S. A. Meenach, K. W. Anderson and J. Z. Hilt, *J. Polym. Sci., Part A: Polym. Chem.*, 2010, **48**, 3229–3235.
37 N. A. Peppas, P. Bures, W. Leobandung and H. Ichikawa, *Eur. J. Pharm. Biopharm.*, 2000, **50**, 27–46.
38 K. J. Loh, T.-C. Hou, J. P. Lynch and N. A. Kotov, *J. Nondestr. Eval.*, 2009, **28**, 9–25.
39 E. P. Chan, J. J. Walish, E. L. Thomas and C. M. Stafford, *Adv. Mater.*, 2011, **23**, 4702–4706.

